JACS
JOURNAL OF THE AMERICAN CHEMICAL SOCIETY

Article

pubs.acs.org/JACS

Single Fluorescent Probe Responds to H_2O_2, NO, and H_2O_2/NO with Three Different Sets of Fluorescence Signals

Lin Yuan, Weiying Lin,* Yinan Xie, Bin Chen, and Sasa Zhu

State Key Laboratory of Chemo/Biosensing and Chemometrics, College of Chemistry and Chemical Engineering, Hunan University, Changsha 410082, P. R. China

Supporting Information

ABSTRACT: Hydrogen peroxide (H_2O_2) acts as a signaling molecule in a wide variety of signaling transduction processes and an oxidative stress marker in aging and disease. However, excessive H_2O_2 production is implicated with various diseases. Nitric oxide (NO) serves as a secondary messenger inducing vascular smooth muscle relaxation. However, mis-regulation of NO production is associated with various disorders. To disentangle the complicated inter-relationship between H_2O_2 and NO in the signal transduction and oxidative pathways, fluorescent reporters that are able to display distinct signals to H_2O_2, NO, and H_2O_2/NO are highly valuable. Herein, we present the rational design, synthesis, spectral properties, and living cell imaging studies of **FP-H_2O_2-NO**, the first single-fluorescent molecule, that can respond to H_2O_2, NO, and H_2O_2/NO with three different sets of fluorescence signals. **FP-H_2O_2-NO** senses H_2O_2, NO, and H_2O_2/NO with a fluorescence signal pattern of blue−black−black, black−black−red, and black−red−red, respectively. Significantly, we have further demonstrated that **FP-H_2O_2-NO**, a single fluorescent probe, is capable of simultaneously monitoring endogenously produced NO and H_2O_2 in living macrophage cells in multicolor imaging. We envision that **FP-H_2O_2-NO** will be a unique molecular tool to investigate the interplaying roles of H_2O_2 and NO in the complex interaction networks of the signal transduction and oxidative pathways. In addition, this work establishes a robust strategy for monitoring the multiple ROS and RNS species (H_2O_2, NO, and H_2O_2/NO) using a single fluorescent probe, and the modularity of the strategy may allow it to be extended for other types of biomolecules.

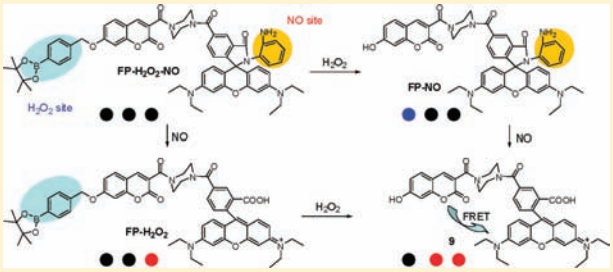

INTRODUCTION

Reactive oxygen species (ROS) are a class of radical or nonradical oxygen-containing species that play critical roles in many physiological and pathological processes.[1] ROS are endogenously generated from oxygen in the mitochondrial respiration pathway.[1a,b] However, under stimulated by xenobiotics, infectious agents, and UV light, ROS can also be exogenously produced.[2] Hydrogen peroxide (H_2O_2), one of the important ROS, acts as a signaling molecule in a wide variety of signaling transduction processes, an oxidative stress marker in aging and disease, and a defense agent in response to pathogen invasion.[3] It is believed that H_2O_2 is generated by activation of NADPH oxidase complexes during cellular stimulation with cytokines, peptide growth factors, and neurotransmitters.[3a] H_2O_2 is involved in reversible oxidation of proteins that ultimately regulate cellular processes ranging from protein phosphorylation to gene expression.[3a] However, excessive H_2O_2 production is implicated with various diseases including cancer, diabetes, and cardiovascular and neurodegenerative disorders.[4]

Reactive nitrogen species (RNS) are another class of chemically reactive species that are essential to many biological functions.[1a,c,d,5] The prototypical RNS is nitric oxide (NO), which is endogenously generated by nitric oxide synthases (NOS), a group of evolutionarily conserved cytosolic or membrane bound isoenzymes that convert L-arginine to citrulline and NO.[5] NO serves as a secondary messenger by activating soluble guanylyl cyclase (sGC), inducing a downstream pathway that elicits vascular smooth muscle relaxation.[6,7] However, mis-regulation of NO production is associated with various diseases ranging from stroke, heart disease, hypertension, neurodegeneration, and erectile dysfunction,to gastrointestinal distress.[7]

Notably, H_2O_2 and NO have interplaying roles in the complex signal transduction and oxidative pathways.[1a,c,d,4a,8−20] H_2O_2 and NO are concurrently present during various physiological processes, and sometimes the generation of H_2O_2 and NO are interdependent.[8] Both H_2O_2 and NO play interrelated roles as signaling molecules during the ABA-dependent stomatal closure.[9] H_2O_2 and NO are synthesized within cardiac myocytes and play important roles in regulating the cardiovascular signaling.[10] A delicate balance between H_2O_2 and NO controls the process of defense against pathogens and decides when the cell death is triggered. Cross-talk between the two signaling molecules is required for the execution of programmed cell death in some living systems. NO can enhance the cytotoxic activity of H_2O_2 in human ovarian cancer

Received: October 25, 2011
Published: December 8, 2011

dx.doi.org/10.1021/ja2100577 | J. Am. Chem.Soc. 2012, 134, 1305−1315

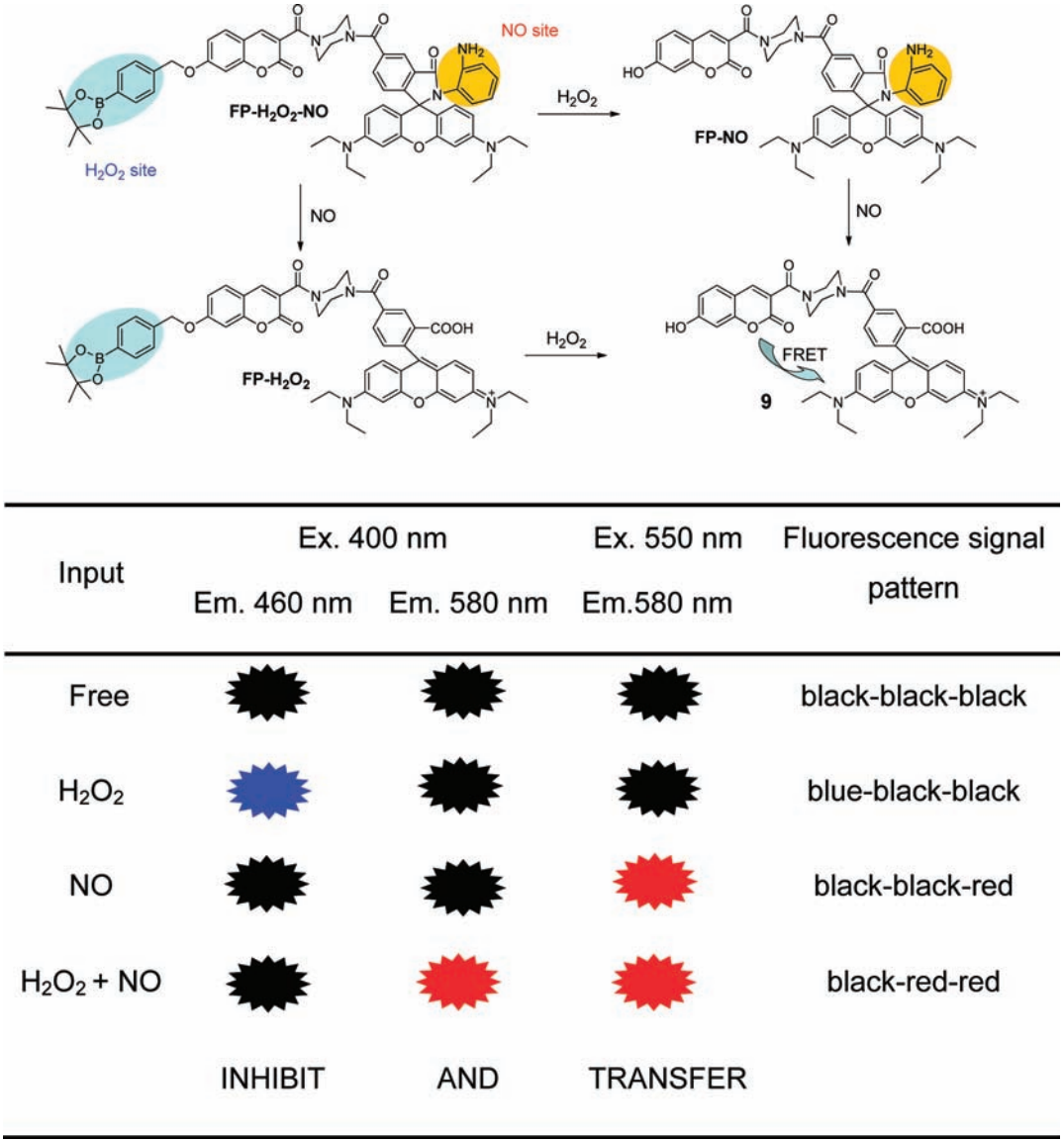

Figure 1. Rational design strategy for probe **FP-H_2O_2-NO**, a unique type of a single fluorescent probe that can report H_2O_2, NO, and H_2O_2/NO with three different sets of fluorescence signals: blue–black–black; black–black–red; and black–red–red.

cells,[11] lymphoma cells,[12] hepatoma cells,[13] and several other types of cells.[14] In contrast, NO inhibits the H_2O_2-induced apoptosis/stress in macrophages,[4a,15] Chinese hamster fibroblasts cells,[16] endothelial cells,[17] and cardiomyoblasts.[18] H_2O_2 can act as an upstream signal to induce production of NO in some animal and plant cells.[8b,c,e,9,10,19] On the other hand, exposure to extracellular NO donor can increase the H_2O_2 level in neuronal cells.[20]

To disentangle the complicated inter-relationship between H_2O_2 and NO in the signal transduction and oxidative pathways, reporters that are able to display distinct signals to H_2O_2, NO, and H_2O_2/NO are highly valuable. An electron spin resonance (ESR)-based method was employed to detect production of ROS and NO in samples of plants and animals.[21] However, this method requires that the biosamples be ground and treated with spin trapping reagents before the ESR measurement can be performed. Thus, the method is destructive and not suitable for monitoring ROS and NO in the native biological environment. By contrast, fluorescence sensing, in combination with microscopy, offers an attractive technique to study biomoleucles of interest in a noninvasive manner with high spatial and temporal resolution.[22] In recent years, a number of well-designed synthetic fluorescent probes specific for H_2O_2[23] or NO[24] have been constructed, and good progress has been made to study H_2O_2 or NO biology by employing these synthetic fluorescent probes. As these fluorescent probes are specific to H_2O_2 or NO, they are not able to respond to H_2O_2, NO, and H_2O_2/NO with three different sets of fluorescence signals. A partial solution to the problem is to use several different types of fluorescent probes in a cell.[10,25] However, as pointed out by Suzuki et al.,[26] the combination of several fluorescent probes produces cross-talk, a larger invasive effect, the different localization, and the different metabolisms, making the scenario very complicated. Thus, a single fluorescent probe which is capable of responding to H_2O_2, NO, and H_2O_2/NO with distinct fluorescence signals is highly desirable for dissecting the complicated roles of these biomolecules in living systems. However, to our best knowledge, the development of such a molecular probe is still an unmet challenge.

dx.doi.org/10.1021/ja2100577 | J. Am. Chem.Soc. 2012, 134, 1305–1315

The aim of our work was to develop a single fluorescent probe based on a 7-hydroxycoumarin−rhodamine platform which can report H_2O_2, NO, and H_2O_2/NO with different fluorescence signal patterns. Thus, the single fluorescent probe can allow H_2O_2, NO, and H_2O_2/NO to be differentiated on the basis of distinct fluorescence responses. Herein, we present the rational design, synthesis, spectral properties, and living cell imaging studies of **FP-H_2O_2-NO** (Figure 1), the first single-fluorescent-molecule, that can respond to H_2O_2, NO, and H_2O_2/NO with three different sets of fluorescence signals. Significantly, **FP-H_2O_2-NO** is capable of simultaneously detecting endogenously produced H_2O_2 and NO in living cells by dual-color fluorescence imaging. **FP-H_2O_2-NO** is promising as a unique molecular tool to report on the production and dynamics of H_2O_2 and NO in the complex interaction networks of the signal transduction and oxidative pathways.

RESULTS AND DISCUSSIONS

Design and Synthesis of Fluorescent Probe FP-H_2O_2-NO and Control Compounds FP-H_2O_2, FP-NO, and 9. Since prominent reports by de Silva et al.,[27] a number of molecular logic gates[28] and fluorescent sensors[29] have been developed by combining multibinding sites and one fluorescent reporter in a single molecule for simultaneous sensing and detection of multianalytes. Inspired by these elegant reports, in this work, we present **FP-H_2O_2-NO** as a new type of single fluorescent probe that can respond to H_2O_2, NO, and H_2O_2/NO with three different sets of fluorescence signals. The design strategy for **FP-H_2O_2-NO** (Figure 1) is formulated based on the following considerations: (1) Selection of the fluorescent dyes. 7-Hydroxycoumarin and rhodamine were chosen as the fluorescent dyes. The absorption wavelengths of 7-hydroxycoumarin and rhodamine dyes are at around 400 and 550 nm (Supporting Information Figure S1), respectively. Thus, their absorption wavelengths are well separated, and they can be independently excited. Furthermore, the emission wavelengths of 7-hydroxycoumarin and rhodamine dyes are at around 460 and 580 nm (Supporting Information Figure S2), respectively. Thereby, their emission wavelengths are essentially resolved, and essentially no cross-talk in the emission spectra is present. This allows them to be employed simultaneously in optical microscopy, key to the success of the two-color imaging of H_2O_2 and NO. (2) Connection of the two fluorescent dyes. 7-Hydroxycoumarin and rhodamine dyes were connected through a rigid piperazine linker. The rigid linker and the relatively short distance (R = 11.07 Å) between the two dyes (Supporting Information Figure S3) ensure their efficient Förster resonance energy transfer (FRET) in the 7-hydroxycoumarin−rhodamine platform ($J_{DA} = 3.62 \times 10^{14}$ M^{-1} cm^{-1} nm^4, R_0 = 36.00 Å, E > 99%, see Table S1 and the corresponding Supporting Information). This opens up opportunities for multiple fluorescence signals. (3) Selection of the responsive sites for H_2O_2 and NO. By exploiting the boronate chemistry, Chang's group has developed the H_2O_2-specific fluorescent probes, and they have made significant progress in studies of H_2O_2 biology using the boronate-based fluorescent probes.[30] Thus, the boronate moiety seems biocompatible and is a good candidate for the H_2O_2 reaction site. On the other hand, the phenylenediamine-based reaction site has been utilized in the construction of fluorescent NO probes for biological imaging in living cells.[24a,d] Thereby, we decided to employ the chemospecific phenylenediamine-based chemistry as the responsive site for NO. (4) Positioning of the responsive sites of H_2O_2 and NO. To minimize the potential interference (i.e., steric hindrance) between the two reaction sites, they were rationally placed on the two ends of the **FP-H_2O_2-NO** molecular scaffold. This setting should allow the two reaction sites to be independently operated. (5) Synthetic accessibility. The overall design allows **FP-H_2O_2-NO** to be constructed in a few synthetic steps. (6) Modularity of the design strategy based on the 7-hydroxycoumarin−rhodamine platform. This flexible design allows a wide variety of reaction sites to be incorporated on the 7-hydroxycoumarin−rhodamine platform. We anticipate that the modular nature of the strategy will afford a versatile approach for sensing multiple targets based on a single fluorescent probe.

On the basis of the above design strategy, we reasoned that **FP-H_2O_2-NO** could respond to H_2O_2, NO, and H_2O_2/NO with distinct fluorescence signal patterns by exploiting the unique optical properties of coumarin and rhodamine dyes. Although 7-hydroxycoumarin has significant absorption at around 400 nm, 7-alkoxycoumarin displays minimal absorption at this wavelength. Rhodamine in the spirocyclic form has essentially no absorption at around 550 nm and is almost nonfluorescent, whereas rhodamine in the open form exhibits intense absorption at around 550 nm and is highly fluorescent. Thus, owing to the characteristic optical properties of coumarin and rhodamine dyes, the free **FP-H_2O_2-NO** has no emission at 460 and 580 nm when excited at 400 nm and no emission at 580 nm when excited at 550 nm. The fluorescence signal pattern for the free probe is black−black−black as shown in Figure 1. However, when the probe is incubated with H_2O_2, the boronate group of **FP-H_2O_2-NO** is removed to afford compound **FP-NO**, which contains the 7-hydroxycoumarin dye and the rhodamine in the spirocyclic form. **FP-NO** has intense emission at 460 nm when excited at 400 nm and exhibits no emission at 580 nm when excited at 400 or 550 nm. Thus, the fluorescence signal pattern for the probe in the presence of H_2O_2 is blue−black−black. Upon treatment of the probe **FP-H_2O_2-NO** with NO, the phenylenediamine group of **FP-H_2O_2-NO** is eliminated to give compound **FP-H_2O_2**, which bears the 7-alkoxycoumarin dye and the rhodamine in the open form. **FP-H_2O_2** has no emission at 460 and 580 nm when excited at 400 nm and exhibits strong emission at 580 nm when excited at 550 nm. Thereby, the fluorescence signal pattern for the probe **FP-H_2O_2-NO** in the presence of NO is black−black−red. When the probe **FP-H_2O_2-NO** is incubated with H_2O_2/NO, the boronate and phenylenediamine groups of **FP-H_2O_2-NO** are removed to eventually provide compound **9**, which contains the 7-hydroxycoumarin dye and the rhodamine dye in the open form. When compound **9** (the 7-hydroxycoumarin−rhodamine platform) is excited at 400 nm, the emission of 7-hydroxycoumarin should transfer to the rhodamine dye by FRET (see Table S1 and the corresponding Supporting Information). Thus, compound **9** has no emission at 460 nm when excited at 400 nm and displays strong emission at 580 nm when excited at 400 or 550 nm. Thus, the fluorescence signal pattern for the probe in the presence of H_2O_2/NO is black−red−red. Taken together, remarkably, a single molecular probe, **FP-H_2O_2-NO**, may respond to H_2O_2, NO, and H_2O_2/NO with three different sets of fluorescence signals: an INHIBIT logic gate at 460 nm when excited at 400 nm and an AND or TRANSFER logic gate at 580 nm when excited at 400 or 550 nm, respectively. This should serve as the basis for independently or simultaneously detection of these

dx.doi.org/10.1021/ja2100577 | J. Am. Chem.Soc. 2012, 134, 1305−1315

Scheme 1. Synthesis of the Probe FP-H_2O_2-NO and the Control Compounds FP-H_2O_2, FP-NO, and 9[a]

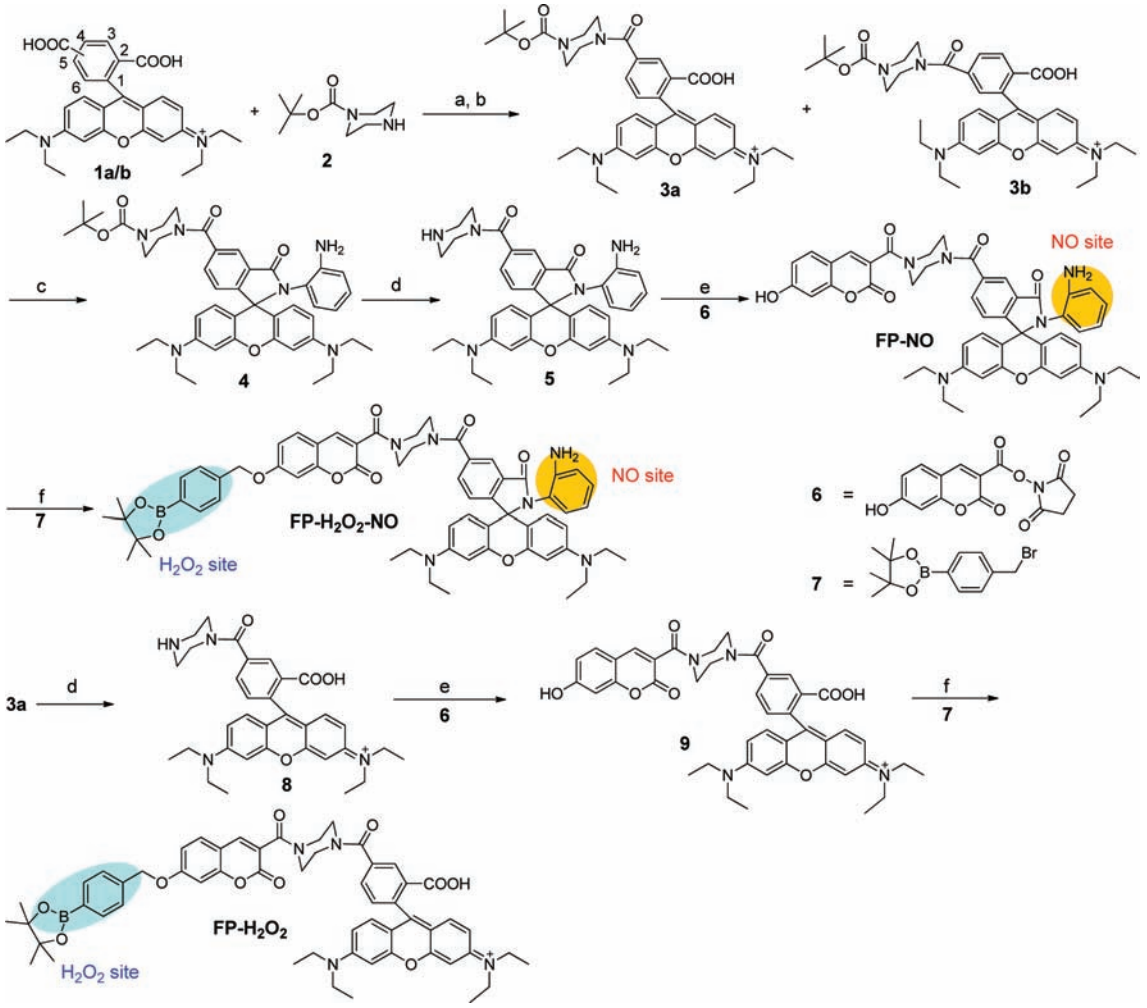

[a]Reagents and conditions: (a) DCC, DMAP, CH_2Cl_2; (b) separation by column chromatography on silica (CH_2Cl_2:CH_3OH = 9:1); (c) DCC, NHS, then benzene-1,2-diamine, $N(Et)_3$; (d) HCl/CH_2Cl_2, then $N(Et)_3$, CH_2Cl_2; (e) $N(Et)_3$, CH_2Cl_2; (f) CH_2Cl_2, Cs_2CO_3.

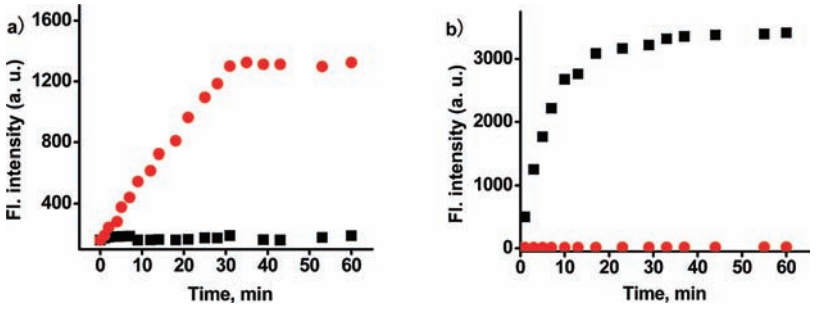

Figure 2. (a) Fluorescence intensity at 586 nm of the control compound **FP-H_2O_2** in the presence of H_2O_2 (●) or NO (■) excited at 400 nm. (b) The fluorescence intensity at 586 nm of the control compound **FP-NO** in the presence of NO (■) or H_2O_2 (●) excited at 550 nm.

key biomolecules in the signal transduction and oxidative pathways.

The synthesis of probe **FP-H_2O_2-NO** started with the preparation of the intermediate **3a** (Scheme 1). Condensation of *t*-Boc-piperazyl **2** with the mixture of 4′- and 5′-carboxyrhodamines **1a**/**b** by the standard coupling chemistry afforded the mixture of **3a**/**b**, which was separated by silica gel column chromatography to give the individual compounds **3a** and **3b** in the pure isomeric form. Treatment of **3a** with coupling reagents N-Hydroxysuccinimide (NHS) and N, N′-Dicyclohexyl carbodiimide (DCC) in CH_2Cl_2 led to the formation of an activated intermediate, which was further reacted with benzene-1,2-diamine to afford the intermediate **4**. Subsequently, the *t*-Boc protecting group of compound **4** was removed under acidic conditions to yield amine **5**, which was then condensated with the activated coumarin **6** under the standard coupling conditions to provide the control compound **FP-NO**. Finally, the hydroxyl group of **FP-NO** was alkylated with bromine **7** to give the probe **FP-H_2O_2-NO**. Control compounds **9** and **FP-H_2O_2** were also prepared in a few steps. The *t*-Boc protecting

dx.doi.org/10.1021/ja2100577 | *J. Am. Chem.Soc.* 2012, 134, 1305−1315

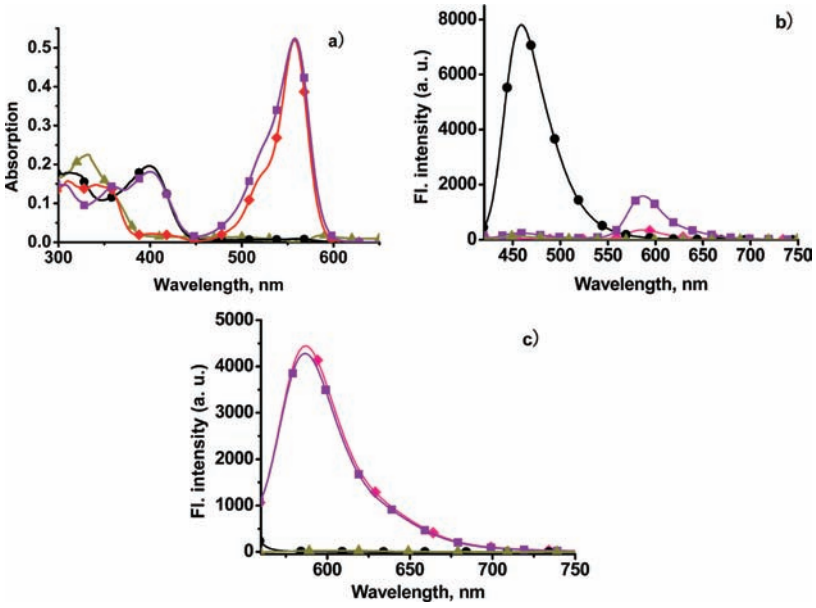

Figure 3. Absorption (a) and emission (b, c) spectra of compounds **FP-H_2O_2-NO** (▲), **FP-H_2O_2** (◆), **FP-NO** (●), and **9** (■) excited at 400 nm (b) or 550 nm (c).

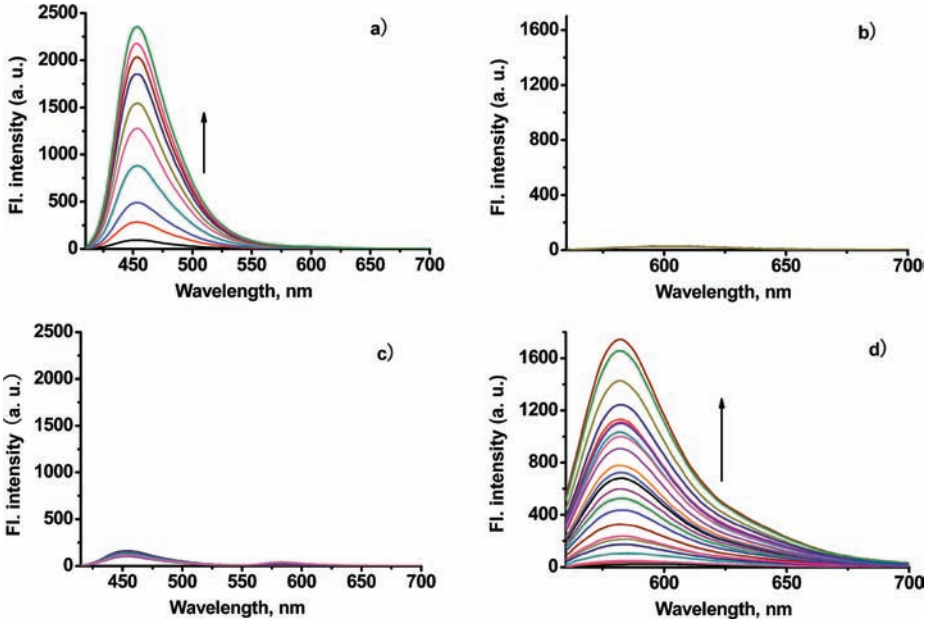

Figure 4. (a, b) Emission spectra of **FP-H_2O_2-NO** (1 μM) in the presence of different equivalents of H_2O_2 (0−50 equiv) excited at 400 nm (a) or 550 nm (b); (c, d) The emission spectra of **FP-H_2O_2-NO** (1 μM) in the presence of different equivalents of NO (0−200 equiv) excited at 400 nm (c) or 550 nm (d).

group of compound **3a** was removed under acidic conditions to yield amine **8**, which was then coupled with the activated coumarin **6** to produce control compound **9** (the 7-hydroxycoumarin−rhodamine platform). Alkylation of the key intermediate **9** afforded another control compound, **FP-H_2O_2**. The structures of **FP-H_2O_2-NO** and control compounds **FP-H_2O_2**, **FP-NO**, and **9** were characterized by ^{1}H NMR, ^{13}C NMR, MS (ESI), and HRMS (ESI).

Investigation of Spectral Properties of FP-H_2O_2-NO. We first decided to examine the selectivity of the boronate-based and phenylenediamine-based reaction sites to H_2O_2 and NO by using control compounds **FP-H_2O_2** and **FP-NO** (their structures are shown in Figure 1 and Scheme 1). As shown in Figure 2a, **FP-H_2O_2** displays a large turn-on fluorescence response in the presence of H_2O_2, whereas it exhibits essentially no fluorescence response to NO, indicating that the boronate-based reaction site is highly selective for H_2O_2 over NO. As displayed in Figure 2b, treatment of **FP-NO** with NO elicits intense emission. By contrast, **FP-NO** has only minimal fluorescence in the presence of H_2O_2, suggesting that the phenylenediamine-based reaction site has high selectivity to NO over H_2O_2. Taken together, these data imply that the boronate-based and phenylenediamine-based reaction sites could appropriately operate in the presence of H_2O_2 or NO, respectively, critical to the success of the probe **FP-H_2O_2-NO**.

dx.doi.org/10.1021/ja2100577 | J. Am. Chem.Soc. 2012, 134, 1305−1315

The spectral properties of the free probe **FP-H_2O_2-NO** were then investigated. As shown in Figure 3a, **FP-H_2O_2-NO** has a featured absorption peak at around 330 nm. However, it has no absorption at around 400 nm as the 7-hydroxyl group of the coumarin dye is alkylated. By sharp contrast, the control compounds **9** and **FP-NO** have significant absorption at 400 nm. Furthermore, the free probe **FP-H_2O_2-NO** displays no marked absorption at around 558 nm, as the rhodamine dye is in the spirocyclic form. However, the control compounds **9** and **FP-** H_2O_2 have strong absorption at 558 nm, as their rhodamine dye is in the open form. Upon excitation at 400 nm, the free probe **FP-H_2O_2-NO** is almost nonfluorescent (Figure 3b). By contrast, the control **FP-NO** has strong emission at 460 nm, ascribed to the fluorescence of 7-hydroxycoumarin dye. Upon excitation at 400 nm, the control **9** has an emission peak at 580 nm, attributed to the emission of the rhodamine dye, as the excited energy is transferred from the 7-hydroxycoumarin to rhodamine dye by FRET. As shown in Figure 3c, upon excitation at 550 nm, the free probe **FP-H_2O_2-NO** is almost nonfluorescent, as its rhodamine dye is in the spirocyclic form. However, the controls **9** and **FP-H_2O_2** exhibit a characteristic emission peak of rhodamine at 580 nm, as their rhodamine dye is in the open form. Thus, the dramatic distinctions in the optical properties of the free probe **FP-H_2O_2-NO** and the controls **9**, **FP-H_2O_2**, and **FP-NO** pave the way for **FP-H_2O_2-NO** to respond to H_2O_2, NO, and H_2O_2/NO with three different sets of fluorescence signals.

The titrations of the probe **FP-H_2O_2-NO** (1 μM) with NO or H_2O_2 was conducted in pH 7.4 PBS buffer with 20% CH_3CN. As shown in Figure 4a, addition of gradually increasing concentrations of H_2O_2 elicits intense emission at around 460 nm when excited at 400 nm. By contrast, no significant emission at 581 nm was observed with excitation at 400 (Figure 4a) or 550 nm (Figure 4b). Thus, in the presence of H_2O_2, **FP-H_2O_2-NO** displays a fluorescence signal pattern of blue−black−black, consistent with that shown in the design scheme (Figure 1). On the other hand, when the probe was incubated with NO, a large fluorescence turn-on at 581 nm was noted upon excitation at 550 nm (Figure 4d). However, no marked fluorescence variations at 460 and 581 nm were detected with excitation at 400 nm (Figure 4c). Thereby, in the presence of NO, **FP-H_2O_2-NO** exhibits a fluorescence signal pattern of black−black−red, in accordance with that shown in the design scheme (Figure 1). These data indicate that the boronate-based and phenylenediamine-based reaction sites of the probe **FP-H_2O_2-NO** selectively responded to H_2O_2 and NO, respectively, as anticipated. It is worth noting that H_2O_2 and NO induce the formation of the emission peaks at 460 and 581 nm, respectively. Thus, the large difference in the emission wavelengths, up to 121 nm, enables them to be suitable for dual-color imaging of H_2O_2 and NO in tandem. The observed rate constants of the probe to H_2O_2 and NO were determined as 3.02×10^{-3} s^{-1} (Supporting Information Figure S4) and 1.18×10^{-3} s^{-1} (Supporting Information Figure S5), respectively, under the pseudo-first-order conditions.

We then investigated the fluorescence response of **FP-H_2O_2-NO** in the presence of H_2O_2 and NO. As it is reported that H_2O_2 can act as an upstream signal to induce production of NO in some animal and plant cells,[8b,c,e,9,10,19] we were interested to know the fluorescence pattern of the probe when successively treated with H_2O_2 and NO. As shown in Figure 5, addition of H_2O_2 to **FP-H_2O_2-NO** triggers a large fluorescence enhancement at 460 nm with excitation at 400 nm. However, the emission intensity at 581 nm with excitation at 400 or 550 nm is almost no variation. These data are consistent with the conversion of **FP-H_2O_2-NO** to **FP-NO** upon addition of H_2O_2 as shown in the design scheme (Figure 1). At the time point of 20 min, NO was further introduced to the solution. A significant enhancement of fluorescence intensity at 581 nm with excitation at 400 or 550 nm and a drastic drop of fluorescence intensity at 460 nm with excitation at 400 nm was observed, in good agreement with the transformation of **FP-NO** to **9** upon further addition of NO (Figure 1). Thus, in the presence of H_2O_2 and NO, **FP-H_2O_2-NO** could ultimately exhibit a fluorescence signal pattern of black−red−red, in good agreement with that shown in the design scheme (Figure 1).

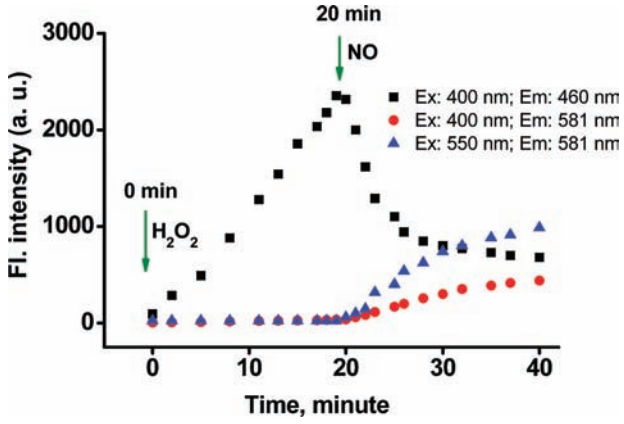

Figure 5. Time-dependent fluorescence intensity of **FP-H_2O_2-NO** at 460 nm excited at 400 nm (■), at 581 nm excited at 400 nm (●), and at 581 nm excited at 550 nm (▲). Notably, H_2O_2 (50 μM) was introduced to **FP-H_2O_2-NO** (1 μM) at 0 min, and then NO (100 μM) was further added at 20 min.

To examine the selectivity, the probe **FP-H_2O_2-NO** was incubated with various reactive oxygen species, reactive nitrogen species, and other biologically relevant species represented by hydrogen peroxide (H_2O_2), hypochlorous acid (HOCl), superoxide ($O_2^{\bullet-}$), hydroxyl radical ($OH^{\bullet}$), *tert*-butyl hydroperoxide (TBHP), *tert*-butoxy radical ($^{\bullet}OtBu$), NO, NO_3^-, NO_2^-, ascorbic acid (AA), and dehydroascorbic acid (DHA) at 100 μM. As shown in Figure 6a, upon excitation at 400 nm, H_2O_2 induces a large fluorescence enhancement at 460 nm, whereas HOCl, $O_2^{\bullet-}$, and other species trigger a small or minimal fluorescence variation, indicating that the probe is selective to H_2O_2 when monitored at 460 nm with excitation at 400 nm, as the boronate-based reaction site is selectively cleaved by H_2O_2. On the other hand, upon excitation at 550 nm, only NO elicits a significant fluorescence increase at 581 nm (Figure 6b). By contrast, almost no change of fluorescence intensity at 581 nm was noted when the probe was incubated with other species, implying that the probe has a high selectivity to NO when monitored at 581 nm with excitation at 550 nm, as the phenylenediamine-based reaction site is selectively removed by NO. Taken together, these results demonstrate that the probe **FP-H_2O_2-NO** can be employed to separately and simultaneously detect H_2O_2 and NO at the different emission channels. Thus, the probe is promising for dual-color imaging of H_2O_2 and NO in living cells.

Fluorescence Imaging of H_2O_2 and NO in HeLa Cells. We proceeded to evaluate the ability of the probe **FP-H_2O_2-NO** to operate in live cells. HeLa cells incubated with **FP-H_2O_2-NO** (5 μM) for 30 min at 37 °C provide almost no

dx.doi.org/10.1021/ja2100577 | *J. Am. Chem.Soc.* 2012, 134, 1305−1315

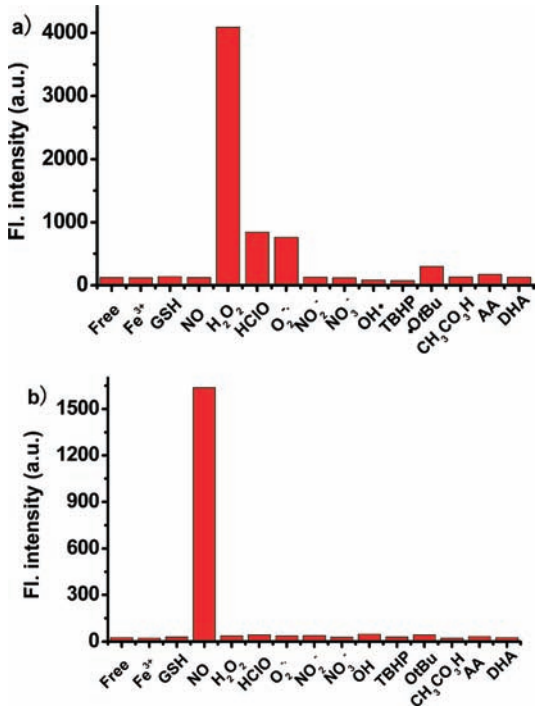

Figure 6. (a) Fluorescence intensity of the probe **FP-H_2O_2-NO** (1 μM) at 460 nm excited at 400 nm in the presence of various biologically relevant species (100 μM). (b) The fluorescence intensity of the probe **FP-H_2O_2-NO** (1 μM) at 581 nm excited at 550 nm in the presence of various biologically relevant species (100 μM).

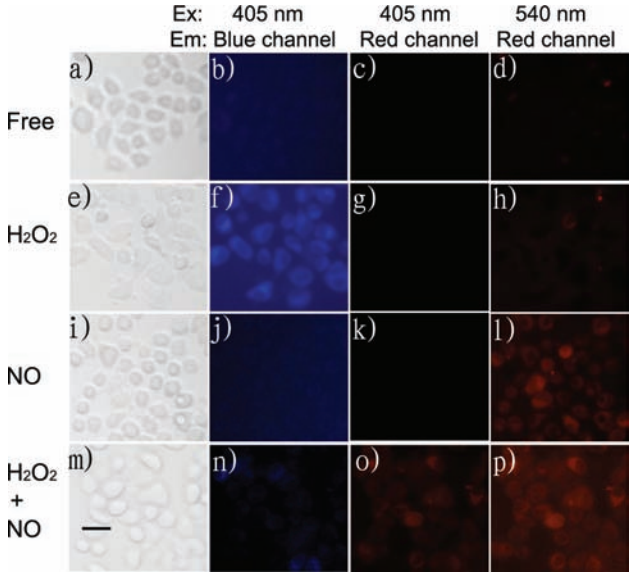

Figure 7. Images of HeLa cells treated with probe **FP-H_2O_2-NO**. (a) Bright field image of HeLa cells incubated with only probe **FP-H_2O_2-NO** (5 μM) for 30 min. (b) Fluorescence image of (a) from blue channel excited at around 405 nm. (c) Fluorescence image of (a) from red channel excited at around 405 nm. (d) Fluorescence image of (a) from red channel excited at around 540 nm. (e) Bright field image of HeLa cells incubated with **FP-H_2O_2-NO** (5 μM) for 30 min and then further incubated with H_2O_2 (50 μM) for another 30 min. (f) Fluorescence image of (e) from blue channel excited at around 405 nm. (g) Fluorescence image of (e) from red channel excited at around 405 nm. (h) Fluorescence image of (e) from red channel excited at around 540 nm. (i) Bright field image of HeLa cells incubated with **FP-H_2O_2-NO** (5 μM) for 30 min and then further incubated with NO donor diethylamine NONOate (50 μM) for another 30 min. (j) Fluorescence image of (i) from blue channel excited at around 405 nm. (k) Fluorescence image of (i) from red channel excited at around 405 nm. (l) Fluorescence image of (i) from red channel excited at around 540 nm. (m) Bright field image of HeLa cells preincubated with **FP-H_2O_2-NO** (5 μM) for 30 min, then treated with H_2O_2 (50 μM) for another 30 min, and further loaded with NO donor diethylamine NONOate (50 μM) for 30 min. (n) Fluorescence image of (m) from blue channel excited at around 405 nm. (o) Fluorescence image of (m) from red channel excited at around 405 nm. (p) Fluorescence image of (m) from red channel excited at around 540 nm. Scale bar = 20 μm.

fluorescence in both the blue channel (Figure 7b) with excitation at around 405 nm and the red channel with excitation at either 405 (Figure 7c) or 540 nm (Figure 7d). However, when the living HeLa cells were loaded with **FP-H_2O_2-NO** and further treated with H_2O_2, they gave strong fluorescence in the blue channel (Figure 7f) and essentially no fluorescence in the red channel with excitation at around 405 nm (Figure 7g) or 540 nm (Figure 7h). These results imply that **FP-H_2O_2-NO** is responsive to H_2O_2 in the living cells. On the other hand, when the living HeLa cells were loaded with **FP-H_2O_2-NO** and then treated with the NO donor diethylamine NONOate, almost no fluorescence in the blue channel (Figure 7j) and the red channel (Figure 7k) with excitation at around 405 nm and a marked increase in the red emission (Figure 7l) on excitation at around 540 nm were observed. These data establish that **FP-H_2O_2-NO** can respond to intracellular NO in living cells. We further examined the ability of **FP-H_2O_2-NO** to respond to H_2O_2 and NO. The living cells were pretreated with **FP-H_2O_2-NO** for 30 min, then incubated with H_2O_2 for another 30 min, and further loaded with the NO donor diethylamine NONOate for 30 min (Figure 7m). Almost no fluorescence in the blue channel (Figure 7n) and a marked increase in the red emission with excitation at around 405 (Figure 7o) or 540 nm (Figure 7p) were detected. Thus, the overall results demonstrate that **FP-H_2O_2-NO** is cell membrane permeable and can monitor intracellular H_2O_2 and NO with three different sets of fluorescence signals as designed (Figure 1).

Fluorescence Imaging of Endogenously Produced H_2O_2 and NO in RAW 264.7 Macrophages Cells. Encouraged by the above promising results, we decided to further examine the feasibility of the probe **FP-H_2O_2-NO** to detect endogenously produced NO and H_2O_2 in a dual-color manner. The RAW264.7 macrophage cells loaded with probe **FP-H_2O_2-NO** display almost no fluorescence in the blue channel (Figure 8b) and the red channel with excitation at around 405 nm (Figure 8c) and 540 nm (Figure 8d). When the RAW264.7 macrophage cells were coincubated with phorbol 12-myristate 13-acetate (PMA) and **FP-H_2O_2-NO** for 1 h, a marked enhancement in the blue channel (Figure 8f) was observed. However, the red channel is almost nonfluorescent (Figures 8g,h). These results are in accordance with the previous reports that PMA can effectively promote H_2O_2 production[31] but induce only slight NO production[32] in RAW264.7 macrophage cells. Thus, the macrophage cells loaded with PMA and **FP-H_2O_2-NO** display a fluorescence pattern of blue–black–black (Figures 8f–h), consistent with that shown in Figure 1 for the probe in the presence of H_2O_2. We then investigated the fluorescence response of the probe when treated with the RAW264.7 macrophage cells prestimulated with lipopolysaccharide (LPS). When the RAW264.7

dx.doi.org/10.1021/ja2100577 | J. Am. Chem.Soc. 2012, 134, 1305–1315

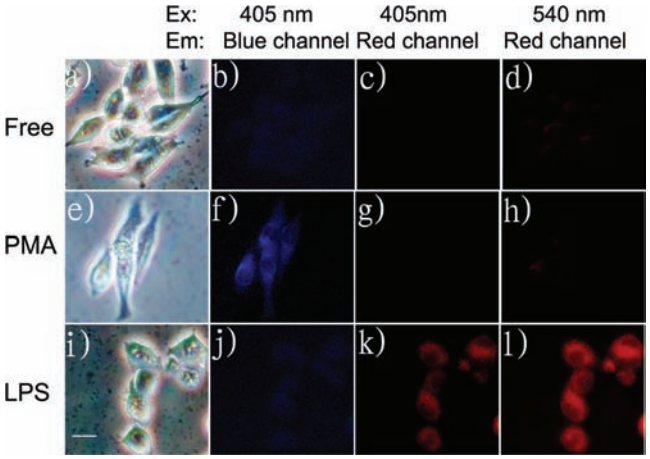

Figure 8. Images of RAW 264.7 macrophages treated with probe **FP-H_2O_2-NO** in the absence or presence of stimulants. (a) DIC image of RAW 264.7 macrophages incubated with only probe **FP-H_2O_2-NO** (5 μM) for 1 h. (b) Fluorescence image of (a) from blue channel excited at around 405 nm. (c) Fluorescence image of (a) from red channel excited at around 405 nm. (d) Fluorescence image of (a) from red channel excited at around 540 nm. (e) DIC image of RAW 264.7 macrophages coincubated with **FP-H_2O_2-NO** (5 μM), PMA (1 μg/mL) for 1 h. (f) Fluorescence image of (e) from blue channel excited at around 405 nm. (g) Fluorescence image of (e) from red channel excited at around 405 nm. (h) Fluorescence image of (e) from red channel excited at around 540 nm. (i) DIC image of RAW 264.7 macrophages incubated with LPS (1 μg/mL) for 12 h and then treated with **FP-H_2O_2-NO** (5 μM) for 1 h. (j) Fluorescence image of (i) from blue channel excited at around 405 nm. (k) Fluorescence image of (i) from red channel excited at around 405 nm. (l) Fluorescence image of (i) from red channel excited at around 540 nm. Notably, the fluorescence responses of the probe in RAW264.7 macrophage cells pretreated with PMA or LPS are in good agreement with those shown in the design scheme (Figure 1). Scale bar = 20 μm.

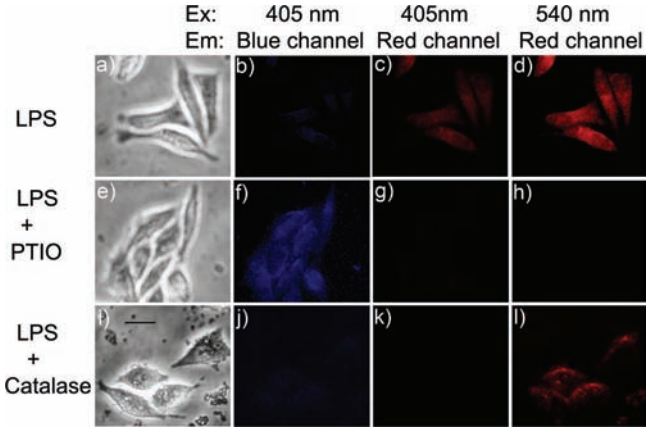

Figure 9. Images of RAW 264.7 macrophages treated with probe **FP-H_2O_2-NO** in the absence or presence of stimulants and scavengers. (a) DIC image of RAW 264.7 macrophage cells incubated with LPS (1 μg/mL) for 12 h and then treated with **FP-H_2O_2-NO** (5 μM) for 1 h. (b) Fluorescence image of (a) from blue channel excited at around 405 nm. (c) Fluorescence image of (a) from red channel excited at around 405 nm. (d) Fluorescence image of (a) from red channel excited at around 540 nm. (e) DIC image of RAW 264.7 macrophages pretreated with LPS (1 μg/mL) for 6 h, then treated with PTIO (a scavenger for NO) for 6 h, and further incubated with **FP-H_2O_2-NO** (5 μM) for 1 h. (f) Fluorescence image of (e) from blue channel excited at around 405 nm. (g) Fluorescence image of (e) from red channel excited at around 405 nm. (h) Fluorescence image of (e) from red channel excited at around 540 nm. (i) DIC image of RAW 264.7 macrophages pretreated with LPS (1 μg/mL) for 6 h, then loaded with PEG-catalase (a scavenger for H_2O_2) for 6 h, and further incubated with **FP-H_2O_2-NO** (5 μM) for 1 h. (j) Fluorescence image of (i) from blue channel excited at around 405 nm. (k) Fluorescence image of (i) from red channel excited at around 405 nm. (l) Fluorescence image of (i) from red channel excited at around 540 nm. Scale bar = 20 μm.

macrophage cells were treated with LPS for 12 h and then incubated with **FP-H_2O_2-NO** for 1 h, essentially no fluorescence in the blue channel (Figure 8j) excited at around 405 nm and a dramatic enhancement in the red emission excited at 405 nm (Figure 8k) or 540 nm (Figure 8l) were detected. These data are in line with the previous reports that LPS can effectively induce the production of both H_2O_2 and NO.[33] Thus, the macrophage cells loaded with LPS and **FP-H_2O_2-NO** exhibit a fluorescence pattern of black–red–red (Figures 8j–l), consistent with that shown in Figure 1 for the probe in the presence of both H_2O_2 and NO, validating the design strategy. Significantly, to our best knowledge, this represents the first report of simultaneous detection of endogenously produced NO and H_2O_2 in dual-color imaging using a single fluorescent probe.

To further confirm that the fluorescence changes of the cells loaded with the probe observed above were indeed induced by H_2O_2 and NO, the living RAW 264.7 macrophages were incubated with **FP-H_2O_2-NO** in the absence or presence of the stimulants and the corresponding scavengers. As anticipated, the cells-loaded with the probe exhibit bright fluorescence in the red channel excited at 405 (Figure 9c) or 540 nm (Figure 9d). However, when the RAW 264.7 macrophages cells were pretreated with LPS (notably, LPS can effectively induce the production of both H_2O_2 and NO[33]) for 6 h, then treated with 2-(4-carboxyphenyl)-4,4,5,5,-tetramethyl-imidazoline-1-oxyl-3-oxide (PTIO), a scavenger for NO,[24e,34] and further loaded with **FP-H_2O_2-NO**, a marked fluorescence enhancement in the blue channel (Figure 9f) and essentially no fluorescence in the red channel (Figures 9g, h) were noted. Comparison of the results of the experiment LPS + PTIO with those of the experiment LPS indicates that the fluorescence variations observed are indeed triggered by NO. On the other hand, when the RAW 264.7 macrophages cells were pretreated with LPS for 6 h, then treated with cell-permeable PEG-catalase, a scavenger for H_2O_2,[35] and further loaded with **FP-H_2O_2-NO**, almost no fluorescence in the blue channel (Figure 9j) and in the red channel with excitation at 405 nm (Figure 9k) and bright fluorescence in the red channel with excitation at 540 nm (Figure 9l) were detected. Comparison of the results of the experiment LPS + catalase with those of the experiment LPS demonstrates that the fluorescence variations observed are indeed triggered by H_2O_2. Thus, taken together, these results establish that **FP-H_2O_2-NO** is capable of simultaneously monitoring endogenously produced NO and H_2O_2 in living macrophage cells in multicolor imaging, suggesting the potential utility of the probe **FP-H_2O_2-NO** in dissecting the interplaying roles of NO and H_2O_2 in the complex interaction networks of the signal transduction and oxidative pathways.

CONCLUSION

In summary, we have described the rational design, synthesis, optical properties, and living cell imaging applications of **FP-H_2O_2-NO**, a unique type of a single fluorescent probe that can report H_2O_2, NO, and H_2O_2/NO with three different sets of

dx.doi.org/10.1021/ja2100577 | J. Am. Chem.Soc. 2012, 134, 1305–1315

fluorescence signals. **FP-H_2O_2-NO** responds to H_2O_2, NO, and H_2O_2/NO with a fluorescence signal pattern of blue−black−black, black−black−red, and black−red−red, respectively. Significantly, we have further demonstrated for the first time that **FP-H_2O_2-NO**, a single fluorescent probe, is capable of simultaneously monitoring endogenously produced NO and H_2O_2 in living macrophage cells in multicolor imaging. We envision that **FP-H_2O_2-NO** will be a unique molecular tool to investigate the interplaying roles of H_2O_2 and NO in many important signaling and oxidative pathways. Further optimization of this class of probes may render new opportunities in studies of complicated ROS and RNS biology. In addition, this work establishes a robust strategy for monitoring the multiple ROS and RNS species (H_2O_2, NO, and H_2O_2/NO) using a single fluorescent probe, and the modularity of the strategy may allow it to be extended for other types of biomolecules by judicious selection of the suitable reaction sites. Work along these lines is under progress. We expect that this type of fluorescent probe may have potential applications in flow cytometry due to the multiple fluorescence signal patterns.

EXPERIMENTAL SECTION

Synthesis of Compound FP-H_2O_2-NO. To a CH_2Cl_2 solution (5 mL) of compound **FP-NO** (40.0 mg, 0.048 mmol) were added compound **7** (43.0 mg, 0.144 mmol) and Cs_2CO_3 (47.0 mg, 0.144 mmol) at room temperature. The mixture was heated and stirred under reflux. After 0.5 h, the solvent was removed under reduced pressure. The resulting residue was subjected to column chromatography on silica (CH_2Cl_2:CH_3OH = 200:1) to yield compound **FP-H_2O_2-NO** as a white solid (34.1 mg, 67.5%). Mp 198−200 °C. ^{1}H NMR ($CDCl_3$, 500 MHz) δ (ppm): 1.15 (t, J = 6.8 Hz, 12H), 1.35 (s, 12H), 3.32−3.91 (16H), 5.17 (s, 2H), 6.09 (d, J = 7.0 Hz, 1H), 6.27 (2H), 6.33 (2H), 6.41 (t, J = 7.5 Hz, 1H), 6.55 (d, J = 8.0 Hz, 1H), 6.64 (2H), 6.89 (s, 1H), 6.93−6.97 (2H), 7.33 (d, J = 7.5 Hz, 1H), 7.43 (d, J = 8.0 Hz, 2H), 7.46 (d, J = 8.5 Hz, 1H), 7.66 (d, J = 8.0 Hz, 1H), 7.84 (d, J = 7.5 Hz, 2H), 7.97 (s, 1H), 8.04 (s, 1H). ^{13}C NMR ($CDCl_3$, 125 MHz) δ (ppm): 12.42, 24.81, 44.36, 70.56, 83.89, 98.02, 101.77, 107.99, 112.07, 114.07, 117.08, 118.25, 120.62, 121.80, 121.88, 125.04, 126.54, 128.54, 128.61, 128.81, 129.83, 131.80, 132.04, 135.17, 138.39, 144.33, 153.83, 156.17, 158.33, 162.98, 164.17, 165.32, 169.73. ESI-MS m/z 1049.5 $[M + H]^+$. HRMS (ESI) m/z calcd for $C_{62}H_{66}{}^{10}BN_6O_9^+$ ($[M + H]^+$): 1048.5024. Found: 1048.5015.

Synthesis of Compound FP-H_2O_2. To a CH_2Cl_2 solution (5 mL) of compound **9** (20.0 mg, 0.027 mmol), were added compound **7** (48.0 mg, 0.16 mmol) and Cs_2CO_3 (44.0 mg, 0.13 mmol) at room temperature, and then the solution was stirred under reflux. After 0.5 h, the solvent was removed under reduced pressure. The resulting residue was subjected to column chromatography on silica (CH_2Cl_2:CH_3OH = 9:1) to yield compound **FP-H_2O_2** as a red powder (12.0 mg, 46.3%). ^{1}H NMR (CD_3OD, 500 MHz) δ (ppm): 1.27 (t, J = 6.5 Hz, 12H), 1.34 (s, 9H), 3.51−3.88 (16H), 5.19 (s, 2H), 6.90−7.02 (5H), 7.22 (s, 2H), 7.36 (2H), 7.44 (d, J = 7.5 Hz, 1H), 7.59 (d, J = 8.5 Hz, 1H), 7.71−7.76 (3H), 8.06 (s, 1H), 8.21 (s, 1H). ^{13}C NMR (CD_3OD, 125 MHz) δ (ppm): 11.47, 23.85, 45.35, 74.46, 83.83, 95.71, 101.41, 112.17, 113.45, 113.63, 113.70, 120.10, 126.34, 126.49, 128.28, 128.67, 129.89, 130.11, 131.56, 134.31, 134.62, 136.49, 139.35, 144.01, 155.49, 156.01, 157.89, 158.74, 160.90, 163.12, 163.20, 165.01, 170.09, 170.69. ESI-MS m/z 959.4 $[M]^+$. HRMS (ESI) m/z calcd for $C_{56}H_{60}{}^{10}BN_4O_{10}^+$ ($[M]^+$): 958.4433. Found: 958.4432.

Synthesis of Compound FP-NO. Compound **5** (50.0 mg, 0.08 mmol) and compound **6** (36.5 mg, 0.12 mmol) were resolved in CH_2Cl_2 (3 mL) at room temperature, and then triethylamine (0.02 mL) was added to the solution with vigorous stirring. After 0.5 h, the solvent was removed under reduced pressure. The resulting residue was subjected to column chromatography on silica (CH_2Cl_2:CH_3OH = 100:1) to give compound **FP-NO** as a white solid (40.1 mg, 60.2%). Mp 214−218 °C (decomposition). ^{1}H NMR (CD_3OD, 500 MHz) δ (ppm): 1.12 (12H), 3.31−3.92 (16H), 5.98 (d, J = 8.0 Hz, 1H), 6.27−6.30 (3H), 6.38 (bs, 2H), 6.58−6.62 (3H), 6.75 (s, 1H), 6.84 (d, J = 8.0 Hz, 1H), 6.91 (t, J = 7.5 Hz, 1H), 7.28 (d, J = 6.0 Hz, 1H), 7.54 (d, J = 7.5 Hz, 1H), 7.72 (d, J = 6.0 Hz, 1H), 8.04 (s, 2H). ^{13}C NMR (CD_3OD, 125 MHz) δ (ppm): 12.81, 45.33, 70.33, 99.19, 103.41, 109.44, 112.46, 115.19, 117.78, 118.29, 120.23, 122.08, 123.02, 126.24, 129.75, 129.88, 130.15, 131.74, 133.17, 133.54, 137.24, 145.83, 146.71, 150.61, 155.29, 155.48, 157.71, 160.45, 164.44, 166.69, 167.43, 171.60. ESI-MS m/z 833.4 $[M + H]^+$. HRMS (ESI) m/z calcd for $C_{49}H_{49}N_6O_7$ ($[M + H]^+$): 833.3617. Found: 833.3657.

HeLa Cells Culture and Imaging. HeLa cells were cultured in Dulbecco's Modified Eagle's Medium (DMEM) supplemented with 10% heat inactivated fetal calf serum (FCS), 2 mM L-glutamine, 50 μg/mL penicillin, and 50 μg/mL streptomycin in an atmosphere of 5% CO_2 and 95% air at 37 °C. One day before imaging, the cells were plated on 6-well plates and allowed to adhere for 24 h. Subsequently, the cells were incubated with **FP-H_2O_2-NO** (5 μM) for 0.5 h at 37 °C and then washed with phosphate-buffered saline (PBS) three times. After incubating with H_2O_2 (50 μM) or NO donor diethylamine NONOate (50 μM) for another 0.5 h at 37 °C, the cells were rinsed with PBS three times, and the fluorescence imaging was performed by an Olympus inverted fluorescence microscope (IX71) equipped with a cooled CCD camera (Figure 7).

Raw 264.7 Murine Macrophages Culture and Imaging. Raw 264.7 murine macrophages were obtained from Xiangya hospital and cultured in DMEM (Dulbecco's Modified Eagle Medium) supplemented with 10% FBS (fetal bovine serum) in an atmosphere of 5% CO_2 and 95% air at 37 °C. For imaging studies, the cells were plated on 6-well plates and allowed to adhere for 24 h. Subsequently, the RAW 264.7 macrophage cells were coincubated with **FP-H_2O_2-NO** (5 μM) and PMA (1 μg/mL) for 1 h in an atmosphere of 5% CO_2 and 95% air at 37 °C. Alternatively, the RAW 264.7 macrophage cells were treated with LPS (1 μg/mL) for 12 h, then loaded with **FP-H_2O_2-NO** (5 μM) for 1 h in an atmosphere of 5% CO_2 and 95% air at 37 °C. Immediately before the experiments, the cells were rinsed with PBS three times, and the fluorescence images were acquired through an Olympus inverted fluorescence microscope (IX71) equipped with a cooled CCD camera (objective magnification: 20-fold, exposition-acquisition times: 400 ms). The culture and imaging experiments in the presence or absence of the stimulants and the corresponding scavengers were conducted in an analogous manner.

ASSOCIATED CONTENT

Supporting Information

Experimental procedures and some spectra. This material is available free of charge via the Internet at http://pubs.acs.org.

AUTHOR INFORMATION

Corresponding Author

weiyinglin@hnu.edu.cn

ACKNOWLEDGMENTS

Funding was partially provided by NSFC (20872032, 20972044, 21172063), NCET (08-0175), the Doctoral Fund of Chinese Ministry of Education (20100161110008), and the Fundamental Research Funds for the Central Universities, Hunan University.

REFERENCES

(1) (a) Bashan, N.; Kovsan, J.; Kachko, I.; Ovadia., H.; Rudich, A. *Physiol. Rev.* **2009**, *89*, 27−71. (b) Kuznetsov, A. V.; Kehrer, I.; Kozlov, A. V.; Haller, M.; Redl, H.; Hermann, M.; Grimm, M.; Troppmair, J. *Anal. Bioanal. Chem.* **2011**, *400*, 2383−2390. (c) Pandey, A. N.; Tripathi, A.; PremKumar, K. V.; Shrivastav, T. G.; Chaube, S. K. *J. Cell. Biochem.* **2010**, *111*, 521−528. (d) Peyrot, F.; Ducrocq, C. *J. Pineal Res.* **2008**, *45*, 235−246.

(2) (a) Gomes, A.; Fernandes, E.; Lima, J. L. F. C. *J. Biochem. Biophys. Methods* **2005**, *65*, 45−80. (b) Caporaso, N. *J. Natl. Cancer Inst.* **2003**, *95*, 1263−1265. (c) Cooke, M. S.; Evans, M. D.; Dizdaroglu, M.; Lunec, J. *FASEB J.* **2003**, *17*, 1195−1214.
(3) (a) Rhee, S. G. *Science.* **2006**, *312*, 1882−1883. (b) Reth, M. *Nat. Immun.* **2002**, *3*, 1129−1134. (c) Rhee, S. G. *Exp. Mol. Med.* **1999**, *31*, 53−59. (d) Stone, J. R.; Yang, S. *Antioxid. Redox. Signaling* **2006**, *8*, 243−270. (e) Winterbourn, C. C. *Nat. Chem. Biol.* **2008**, *4*, 278−286. (f) Paulsen, C. E.; Carroll, K. S. *ACS Chem. Biol.* **2010**, *5*, 47−62. (g) Miller, E. W.; Dickinson, B. C.; Chang, C. J. *Proc. Natl. Acad. Sci. U.S.A.* **2010**, *107* (36), 15681−15686. (h) D'Autréaux, B.; Toledano, M. B. *Nat. Rev. Mol. Cell. Biol.* **2007**, *8*, 813−824. (i) Gough, D. R.; Cotter, T. G. *Cell Death Dis.* **2011**, *2*, e213.
(4) (a) Krohn, K.; Maier, J.; Paschke, R. *Nat. Clin. Pract. Endocrinol. Metab.* **2007**, *3*, 713−720. (b) Galaris, D.; Skiada, V.; Barbouti, A. *Cancer Lett.* **2008**, *266*, 21−29. (c) Lin, M. T.; Beal, M. F. *Nature* **2006**, *443*, 787−795.
(5) (a) Alderton, W. K.; Cooper, C. E.; Knowles, R. G. *Biochem. J.* **2001**, *357*, 593−615. (b) Soneja, A.; Drews, M.; Malinski, T. *Pharmacol. Rep.* **2005**, *57* (suppl), 108−119.
(6) Cary, S. P. L; Winger, J. A.; Derbyshire, E. R.; Marletta, M. A. *Trends Biochem. Sci.* **2006**, *31*, 231−239.
(7) *Nitric Oxide; Handbook of Experimental Pharmacology*; Mayer, B., Ed.; Springer: Berlin, 2000; Vol. *143*.
(8) (a) Milligan, S. A.; Owens, M. W.; Grisham, M. B. *Am. J. Physiol. - Lung Cell* **1996**, *271*, L114−L120. (b) Shiota, K.; Shimizu, S.; Ishii, M.; Yamamoto, S.; Iwasaki, M.; Yamamoto, T.; Kiuchi, Y. *Pteridines* **2002**, *13*, 21−25. (c) Eguchi, H.; Fujiwara, N.; Sakiyama, H.; Yoshihara, D.; Suzuki, K. *Neurosci. Lett.* **2011**, *494*, 29−33. (d) Lum, H. K.; Butt, Y. K. C.; Lo, S. C. L. *Nitric Oxide* **2002**, 205−213. (e) Li, J.-H. *Plant. Physiol.* **2009**, 114−124.
(9) Zhang, A.; Jiang, M.; Zhang, J.; Ding, H.; Xu, S.; Hu, X.; Tan, M. *New. Phytol.* **2007**, *175*, 36−50.
(10) Sartoretto, J. L.; Kalwa, H.; Pluth, M. D.; Lippard, S. J.; Michel, T. *Proc. Natl. Acad. Sci. U.S.A.* **2011**, *108*, 15792−15797.
(11) Yoshioka, Y.; Kitao, T.; Kishino, T.; Yamamuro, A.; Maeda, S. *J. Immunol.* **2006**, *176*, 4675−4681.
(12) Filep, J. G.; Lapierre, C.; Lachance, S.; Chan., J. S. *Biochem. J.* **1997**, *321*, 897−901.
(13) Ioannidis, I.; de Groot, H. *Biochem. J.* **1993**, *296*, 341−345.
(14) (a) Hoffmann, O.; Zweigner, J.; Smith, S. H.; Freyer, D.; Mahrhofer, C.; Dagand, E.; Tuomanen, E. I.; Weber1, J. R. *Infect. Immun.* **2006**, *74*, 5058−5066. (b) Rauen, U.; Li, T.; Ioannidis, I.; de Groot, H. *Am. J. Physiol. Cell. Physiol* **2007**, *292*, C1440−C1449.
(15) Farias-Eisner., R. *J. Biol. Chem.* **1996**, *271*, 6144−6151.
(16) Ridnour, L. A. *Free Radical Biol. Med.* **2005**, *38*, 1361−1371.
(17) Kotamraju, S.; Tampo, Y.; Keszler, A.; Chitambar, C. R.; Joseph, J.; Haas, A. L.; Kalyanaraman, B. *Proc. Natl. Acad. Sci. U.S.A.* **2003**, *100*, 10653−10658.
(18) Chae, H. J.; Kim, H. R.; Kwak, Y. G.; Ko, J. K.; Joo, C. U.; Chae, S. W. *Immunopharmacol. Immunotoxicol.* **2001**, *23*, 187−204.
(19) (a) Milligan, S. A.; Owens, M, W.; Grisham, M. B. *Am. J. Physiol. - Lung Cell.* **1996**, *271*, L114−L120. (b) Lum, H. K.; Butt, Y. K. C.; Lo, S. C. L. *Nitric Oxide* **2002**, 205−213.
(20) Wei, T.; Chen, C.; Hou, J.; Xin, W.; Mori, A. *Biochim. Biophys. Acta* **2000**, *1498*, 72−79.
(21) Cao, Y.; Guo, P.; Xu, Y.; Zhao, B. *Methods Enzymol.* **2005**, *396*, 77−83.
(22) For some reviews, see: (a) Miller, E. W.; Chang, C. J. *Curr. Opin. Chem. Biol.* **2007**, *11*, 620−625. (b) Chen, X.; Tian, X.; Shin, I.; Yoon, J. *Chem. Soc. Rev.* **2011**, *40*, 4783−4804. (c) McQuade, L. E.; Lippard, S. J. *Curr. Opin. Chem. Biol.* **2010**, *14*, 43−49.
(23) For some examples, see: (a) Dickinson, B. C.; Huynh, C.; Chang, C. J. *J. Am. Chem. Soc.* **2010**, *132*, 5906−5915. (b) Srikun, D.; Miller, E. W.; Domaille, D. W.; Chang, C. J. *J. Am. Chem. Soc.* **2008**, *130*, 4596−4597. (c) Abo, M.; Urano, Y.; Hanaoka, K.; Terai, T.; Komatsu, T.; Nagano, T. *J. Am. Chem. Soc.* **2011**, *133*, 10629−10637. (d) Du, L.; Ni, N.; Li, M.; Wang, B. *Tetrahedron Lett.* **2010**, *51*, 1152−1154. (e) Xu, K. H.; Liu, F.; Wang, H. X.; Wang, S. S.; Wang, L. L.; Tang, B. *Sci. China. Ser. B: Chem.* **2009**, *52*, 734−740.
(24) For some examples, see: (a) Gabe, Y.; Urano, Y.; Kikuchi, K.; Kojima, H.; Nagano, T. *J. Am. Chem. Soc.* **2004**, *126*, 3357−3367. (b) McQuade, L. E.; Ma, J.; Lowe, G.; Ghatpande, A.; Gelperin, A.; Lippard, S. J. *Proc. Natl. Acad. Sci. U.S.A.* **2010**, *107*, 8525−8530. (c) Yang, Y.; Seidlits, S. K.; Adams, M. M.; Lynch, V. M.; Schmidt, C. E.; Anslyn, E. V.; Shear, J. B. *J. Am. Chem. Soc.* **2010**, *132*, 13114−13115. (d) Zheng, H.; Shang, G.-Q.; Yang, S.-Y.; Gao, X.; Xu, J.-G. *Org. Lett.* **2008**, *10*, 2357−2360. (e) Sun, C.; Shi, W.; Song, Y.; Chen, W.; Ma, H. *Chem. Commun.* **2011**, *47*, 8638−8640. (f) Wang, J.; He, C.; Wu, P.; Wang, J.; Duan, C. *J. Am. Chem. Soc.* **2011**, *133*, 12402−12405.
(25) For some examples, see: (a) She, X.-P.; Song, X.-G.; He, J.-M. *Acta Bot. Sin.* **2004**, *46*, 1292−1300. (b) Lombardi, L.; Ceccarelli, N.; Picciarelli, P.; Sorce, C.; Lorenzi, R. *Physiol. Plant* **2010**, *140*, 89−102.
(26) Komatsu, H.; Miki, T.; Citterio, D.; Kubota, T.; Shindo, Y.; Kitamura, Y.; Oka, K.; Suzuki, K. *J. Am. Chem. Soc.* **2005**, *127*, 10798−10799.
(27) (a) de Silva, A. P.; Gunaratne, H. Q. N.; McCoy, C. P. *Nature* **1993**, *364*, 42−44. (b) deSilva, A. P.; McClenaghan, N. D. *J. Am. Chem. Soc.* **2000**, *122*, 3965−3966.
(28) For some examples, see: (a) Uchiyama, S.; Kawai, N.; de Silva, A. P.; Iwai, K. *J. Am. Chem. Soc.* **2004**, *126*, 3032−3033. (b) Pischel, U. *Angew. Chem., Int. Ed.* **2007**, *46*, 4026−4040. (c) Qu, D.-H.; Wang, Q.-C.; Tian, H. *Angew. Chem., Int. Ed.* **2005**, *44*, 5296−5299. (d) Margulies, D.; Felder, C. E.; Melman, G.; Shanzer, A. *J. Am. Chem. Soc.* **2007**, *129*, 347−354. (e) Bozdemir, O. A.; Guliyev, R.; Buyukcakir, O.; Selcuk, S.; Kolemen, S.; Gulseren, G.; Nalbantoglu, T.; Boyaci, H.; Akkay, E. U. *J. Am. Chem. Soc.* **2010**, *132*, 8029−8036. (f) Coskun, A.; Deniz, E.; Akkaya, E. U. *Org. Lett.* **2005**, *7*, 5187−5189. (g) Magri, D. C.; Brown, G. J.; McClean, G. D.; de Silva, A. P. *J. Am. Chem. Soc.* **2006**, *128*, 4950−4951. (h) Kumar, S.; Luxami, V.; Saini, R.; Kaur, D. *Chem. Commun.* **2009**, 3044−3046. (i) de Silva, A. P. *Isr. J. Chem.* **2011**, *51*, 16−22. (j) Qian, J.; Qian, X.; Xu, Y. *Chem.—Eur. J.* **2009**, *15*, 319−323. (k) Zhang, L.; Whitfield, W. A.; Zhu, L. *Chem. Commun.* **2008**, 1880−1882. (l) Li, A.-F.; Ruan, Y.-B.; Jiang, Q.-Q.; He, W.-B.; Jiang, Y.-B. *Chem.—Eur. J.* **2010**, *16*, 5794−5802. (m) Rurack, K.; Trieflinger, C.; Kovalchuck, A.; Daub, J. *Chem.—Eur. J.* **2007**, *13*, 8998−9003.
(29) For some examples, see: (a) Srikun, D.; Albers, A. E.; Chang, C. J. *Chem. Sci.* **2011**, *2*, 1156−1165. (b) Rurack, K.; Koval'chuck, A.; Bricks, J. L.; Slominskii, J. L. *J. Am. Chem. Soc.* **2001**, *123*, 6205−6206. (c) Ji, H.-F.; Dabestani, R.; Brown, G. M. *J. Am. Chem. Soc.* **2000**, *122*, 9306−9307. (d) Arosio, D.; Ricci, F.; Marchetti, L.; Gualdani, R.; Albertazzi, L.; Beltram, F. *Nat. Med.* **2010**, *7*, 516−518. (e) Li, Y.; Wang, H.; Li, J.; Zheng, J.; Xu, X.; Yang, R. *Anal. Chem.* **2011**, *83*, 1268−1274. (f) Yang, X.; Guo, Y.; Strongin, R. M.. *Angew. Chem., Int. Ed.* **2011**, *50*, 10690−10693. (g) Xing, Z.; Wang, H.-C.; Cheng, Y.; James, T. D.; Zhu, C. *Chem. Asian J.* **2011**, *6*, 3054−3058. (h) Tulyakova, E.; Delbaere, S.; Fedorov, Y.; Jonusauskas, G.; Moiseeva, A.; Fedorova, O. *Chem.—Eur. J.* **2011**, *17*, 10752−10762.
(30) Lippert, A. R.; Van de Bittner, G. C.; Chang, C. J. *Acc. Chem. Res.* **2011**, *44*, 793−804.
(31) (a) Li, H.; Li, Q.; Wang, X.; Xu, K.; Chen, Z.; Gong, X.; Liu, X.; Tong, L.; Tang, B. *Anal. Chem.* **2009**, *81*, 2193−2198. (b) Gong, X.; Li, Q.; Xu, K.; Liu, X.; Li, H.; Chen, Z.; Tong, L.; Tang, B.; Zhong, H. *Electrophoresis* **2009**, *30*, 1983−1990.
(32) Chen, F.; Kuhn, D. C.; Gaydos, L. J.; Demers, L. M. *APMIS* **1996**, *104*, 176−182.
(33) (a) Lee, S.-J.; Lim, K.-T. *Naunyn-Schmiedeberg's Arch. Pharmacol.* **2008**, *377*, 45−54. (b) Park, S. Y.; Ji, G. E.; Ko, Y. T.; Jung, H. K.; Ustunol, Z.; Pestka, J. J. *Int. J. Food Microbiol.* **1999**, *46*, 231−241. (c) Lee, I.; Hwang, O.; Yoo, D.; Khang, G.; Lee, D. *Bull. Korean Chem. Soc.* **2011**, *32*, 2187−2192. (d) Lee, D.; Khaja, S.; Velasquez-Castano, J. C.; Dasari, M.; Sun, C.; Petros, J.; Taylor, W. R.; Murthy, N. *Nat. Mater.* **2007**, *6*, 765−769. (e) Hikosaka, K.; Koyama, Y.; Motobu, M.; Yamada, M.; Nakamura, K.; Koge, K.; Shimura, K.; Isobe, T.; Tsuji, N.;

Kang, C. B.; Hayashidani, H.; Wang, P. C.; Matsumura, M.; Hirota, Y. *Biosci. Biotechnol. Biochem.* **2006**, *70*, 2853.−2858.
(34) Roy, A.; Fung, Y. K.; Liu, X. J.; Pahan, K. *J. Biol. Chem.* **2006**, *281*, 14971−14980.
(35) (a) Beckman, J. S.; Minor, R. L.; White, C. W.; Repine, J. E.; Rosen, G. M.; Freeman, B. A. *J. Biol. Chem.* **1988**, *263*, 6884−6892. (b) Cogolludo, A.; Frazziano, G.; Cobeño, L.; Moreno, L.; Lodi, F.; Villamor, E.; Tamargo, J.; Perez-Vizcaino, F. *Ann. N. Y. Acad. Sci.* **2006**, *1091*, 41−51.